RSC Advances

Synthesis, characterization, DNA interaction of novel Pt(Ⅱ) complexes and their cytotoxicity, apoptosis and molecular docking

SCHOLARONE™
Manuscripts

ARTICLE

Synthesis, characterization, DNA interaction of novel Pt(II) complexes and their cytotoxicity，apoptosis and molecular docking

MingChang Zhu[a,b,c], Xiaoting Cui[d], FuChen Zhao[b,c], Xiaoyu Ma[b,c]，ZhengBo Han[a*], EnJun Gao[b,c*]

The complexes $[Pt\{Ar(COOH)_2\}(OH)_2]$ (1), $[Pt\{Ar(COOH)_2\}(OH)_2]\cdot H_2O$ (2) have been synthesized and characterized by IR, ^{1}H NMR, element analysis and single-crystal X-ray diffractometry. The interaction of the Pt(II) complexes with fish sperm DNA was explored by UV absorption, fluorescence spectroscopy and viscosity measurements. The results indicated that the complexes bind to FS-DNA in an intercalative mode with different binding affinity. The reaction of the complexes with N7, N3/ N9 from the guanine and adenine were investigated by ^{1}H NMR. Gel electrophoretic assay demonstrated the ability of the Pt(II) complexes to cleave the pBR322 plasmid DNA. The docking methods were used to predict the DNA binding affinity of Pt(II) complexes by the resulting relative binding energy with DNA with -6.74 kcal/mol (complex 1) and -6.21 kcal/mol (complex2). The cytotoxic activity of the complexes was tested against Hela cancer cell lines. The two complexes showed cytotoxic specificity and significant cancer cell inhibitory rate. Complex 1 possessed the highest inhibition on viability of tested cells. Furthermore, the apoptotic tests indicated that the complexes had an apoptotic effect on HeLa cells.

Introduction

[a.] *College of Chemistry, Liaoning University, Shenyang 110036 P. R. China*
[b.] *Department of Coordination Chemistry, Shenyang University of Chemical Technology, Shenyang 110142, P.R.China*
[c.] *International Key Laboratory of Shenyang Inorganic Molecule-Based Chemical, Shenyang, 110142, P.R. China*
[d.] *. School of chemical engineering，Tianjin University, Tianjin 300072 P.R.China*
† Footnotes relating to the title and/or authors should appear here.
Electronic Supplementary Information (ESI) available: [details of any supplementary information available should be included here]. See DOI: 10.1039/x0xx00000x

Cisplatin (cis-diamminedichloroplatinum(II) is currently used clinically and is one of the most effective anticancer drugs in the treatment of a variety of human tumors. [1,2] Unfortunately, the clinical use of cisplatin is restricted by nephrotoxicity, peripheral neuropathy, liver toxicity, myelotoxicity, gastrointestinal toxicity, and ototoxicity.[3,4] Therefore, a number of cisplatin analogues have been synthesized and characterized with

equal or greater antitumor activity but lower toxicity.[5–6] Even though the biological activity of cisplatin analogues has been ascribed to different signaling pathways, in fact it is primarily related to its interaction with chromosomal DNA by means of inter- or intrastrand cross-linking and DNA−protein cross-linking as well. [7] And the major platination site of cisplatin is known to be the N7 atom of guanine.[8] DNA binding has been researched in numerous studies[9-11] consisting of research into the kinetics of cross-linking DNA with cisplatin.[11–17] Nowadays, an active research area is focused on the development of new metallodrugs capable of interacting with DNA, and organometallic Pt(II) complexes are promising candidates to this aim.

Based on the structural analogy among transition metal complexes, herein, we report the synthesis and characterization of the two complexes of the general formula $[Pt\ (L)(H_2O)_2]$, where L is an Pyrazine-2,3-dicarboxylic acid or Pyridine-2,3-dicarboxylic acid ligand (Figure.1). The interaction of these complexes with fish sperm DNA (FS-DNA) has been examined via

fluorescence spectroscopy, electronic absorption titration and viscosity experiment. Their cleavage behavior toward pBR322 plasmid DNA, cytotoxicity in vitro and apoptosis were also investigated. The results suggest that the two complexes have potential precursors of the anticancer drug.
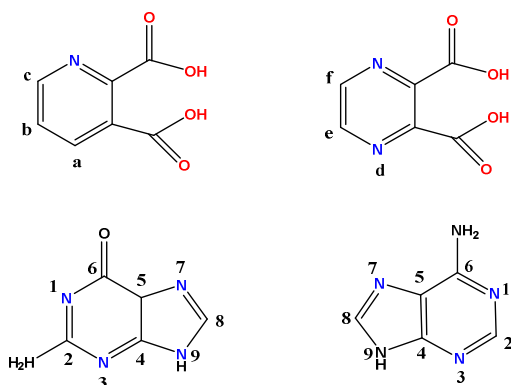
Figure. 1. Schematic structure of the ligands and the numbering scheme for ^{1}H NMR spectroscopy.

Results and discussion

X-ray crystal structure of complex 1: Single-crystal structure of complex **1** was determined by X ray crystallography as shown in Figure 2, and with atom numbering scheme. Selected bond lengths (Å) and angles (deg) are shown in Table 1.

Table 1 Selected bond lengths (Å) and angels (deg) for complex 1 and**2.**

Complex 1			
Pt(1)-N(1)	2.004(4)	Pt(1)-O(4)	2.020(4)
Pt(1)-O(6)	2.041(4)	Pt(1)-O(5)	2.045(4)
N(1)-Pt(1)-O(4)	81.56(14)	N(1)-Pt(1)-O(6)	96.39(16)
N(1)-Pt(1)-O(5)	174.16(16)	O(4)-Pt(1)-O(6)	176.47(16)
O(4)-Pt(1)-O(5)	93.15(16)	O(6)-Pt(1)-O(5)	89.02(17)
C(4)-N(1)-Pt(1)	127.9(3)	C(1)-N(1)-Pt(1)	112.5(3)
C(5)-O(4)-Pt(1)	114.5(3)	C(3)-N(2)-C(2)	117.1(4)
C(4)-N(1)-C(1)	119.6(4)	N(1)-C(1)-C(2)	119.5(4)
Complex 2**.**			
Pt(1)-N(1)	1.999(4)	Pt(1)-O(1)	2.033(4)
Pt(1)-O(1W)	2.040(5)	Pt(1)-O(2W)	2.044(4)
N(1)-Pt(1)-O(1)	81.02(16)	N(1)-Pt(1)-O(1W)	96.92(17)
N(1)-Pt(1)-O(2W)	175.37(18)	O(1)-Pt(1)-O(1W)	177.83(16)
O(1)-Pt(1)-O(2W)	94.41(17)	O(1W)-Pt(1)-O(2W)	87.66(18)
C(6)-O(1)-Pt(1)	115.6(3)	C(1)-N(1)-Pt(1)	114.4(3)
C(5)-N(1)-Pt(1)	127.2(4)	C(1)-N(1)-C(5)	118.4(4)
N(1)- C(5) -C(4)	119.6(5)	N(1)-C(1)-C(2)	120.8(4)

As shown in Figure 2, the platinum atom is coordinated with the N(1) and O(4), which come from the L_1 ligand and the O(5) and O(6) from two water molecules. The (N(1)-Pt(1)-O(5)) angle is 174.16°and the (O(4)-Pt(1)-O(6)) angle is 176.47°, and therefore the coordination geometry of the Pt atom is square planar with rather
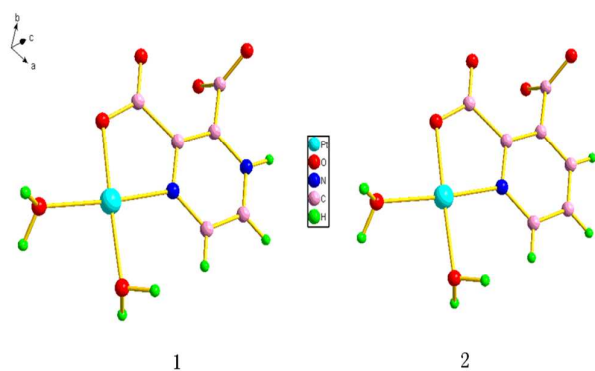
Figure.2. The independent molecule of the two title complexes with numbering of atoms at 30% probability thermal ellipsoids.

small deviations of the ligating atoms from the coordination plane. The L_1 ligands are stacked (centroid-to-centroid distances of 3.827 Å, shown in Figure. 3.) in a face-to-face mode, conforming to an approximate interaction.[18]
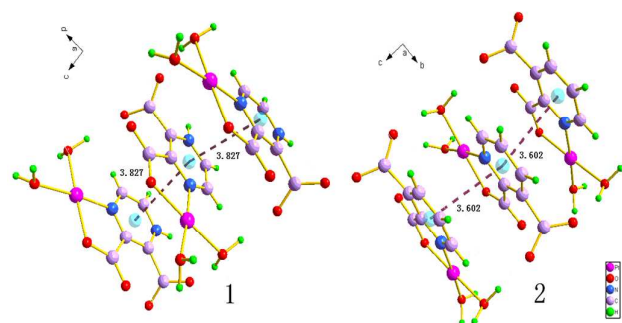
Figure. 3. The one-dimension chains of **1** and **2** through the π-π weak interaction.

Crystallographic structure of complex 2: The crystal structure of complex **2** was measured by X ray crystalography as shown in Figure. 2. Table 1 lists selected interatomic distances (Å) and angles (deg). Crystal data and structure refinement details are summarized in Table 2.

Table **2** Crystal data and refinement for complex 1 and 2

Empirical formula	$C_6 H_6 N_2 O_6 Pt$	$C_7 H_9 N O_7 Pt$
Formula weight	397.22	414.24
Temperature (K)	293(2)	293(2)
Wavelength (Å)	0.71073	0.71073
Crystal system	Monoclinic	Monoclinic
Space group	P2(1)/c	P2(1)/c
a (Å)	8.2784(10)	7.6445(17)
b (Å)	7.0371(9)	18.415(4)
c (Å)	16.043(2)	7.1370(16)
α (deg)	90	90
β (deg)	99.097(2)	96.371(3)
γ (deg)	90	90
Volume (Å³)	922.9(2)	998.5(4)
Z	4	4
Dcalc (mg/m³)	2.859	2.756
Absorption coefficient (mm⁻¹)	15.217	14.075
F(000)	728	768
Crystal size	0.10 x 0.08 x 0.06	0.31 x 0.10 x 0.09
θ Range for data collection (deg)	2.49–25.38	2.21–25.66
Index ranges	-8≤h≤9,-7≤k≤8,-18≤l≤19	-9≤h≤7,-20≤k≤22,-8≤l≤8
Reflections collected	4657	5365
Independent reflections (Rint)	1684(0.0186)	1882(0.0224)
Data/restraints/parameters	1684 / 0 / 152	1882 / 9 / 163
S	1.037	1.033
Final R indices [I > 2σ(I)]	R1=0.0182,wR2=0.0460	R1 = 0.0217,wR2 = 0.0536
R indices (all data)	R1=0.0201,wR2=0.0469	R1 = 0.0253,wR2 = 0.0555
Largest diffraction peak and hole(Å e³)	1.012 and -0.501	0.901 and -0.692

As can be seen in Figure 2, the platinum atom is coordinated with the N(1) and O(1), which come from the L_2 ligand and the O(1W) and O(2W) from two water molecules. The (N(1)-Pt(1)-O(2W)) angle is 175.37°and the (O(1)-Pt(1)-O(1W)) angle is 177.83°, and so the coordination geometry of the Pt atom is square planar with rather small deviations of the ligating atoms from the coordination plane. The L_2 ligands are stacked

(centroid-to-centroid distances of 3.602 Å, shown in Figure. 3.) in an offset face-to-face mode arrangement by dihedral angle of 2.13°, conforming to an approximate interaction.[19]

Fluorescence spectroscopic studies: Fluorescence quenching measurements can be used to investigate metal binding.[19] The molecular fluorophore ethidium bromide emits intense fluorescent in the presence of DNA due to its strong intercalation between the adjacent DNA base pairs. It had been reported that the enhanced fluorescence could be quenched by the addition of another molecule and quenching of DNA–EtBr fluorescence by the addition complexes causes a reduction in the emission intensity, indicating the competition between the complex and ethidium bromide in binding to DNA.[20,21] The study includes the addition of the complexes to DNA pretreated with ethidium bromide (ethidium bromide/ DNA= 1/5). In Figure 4, the emission spectra of ethidium bromide bound to DNA in the absence and presence of the two complexes are shown. The addition of each Pt(II) complex to DNA pretreated with ethidium bromide brings on an appreciable reduction in fluorescence intensity, indicating that the complexes compete with ethidium bromide to bind with DNA. It is in accordance with the classical Stern–Volmer equation [21]: $I_0/I=1 + K_{sq}r$, where I_0 and I represent the fluorescence intensities in the absence and presence of the complex, respectively, and r is the concentration ratio of the complex to DNA. K_{sq} is a linear Stern–Volmer quenching constant dependent on the ratio of the bound concentration of ethidium bromide to the concentration of DNA. The K_{sq} value is acquired as the slope of I_0/I versus r linear plot. The curve about quenching of DNA–ethidium bromide fluorescence by the two complexes is shown in Figure. 5. From the inset in Figure. 5, the K_{sq} value for the two

complexes is respectively 0.465 and 0.544. Such a value of quenching constant suggests that the interaction of the complex with DNA is of moderate intercalation.[20, 22] Thus, it can be confirmed that the reactions between the two intercalary complexes and the adjacent DNA base pairs have taken place[23].
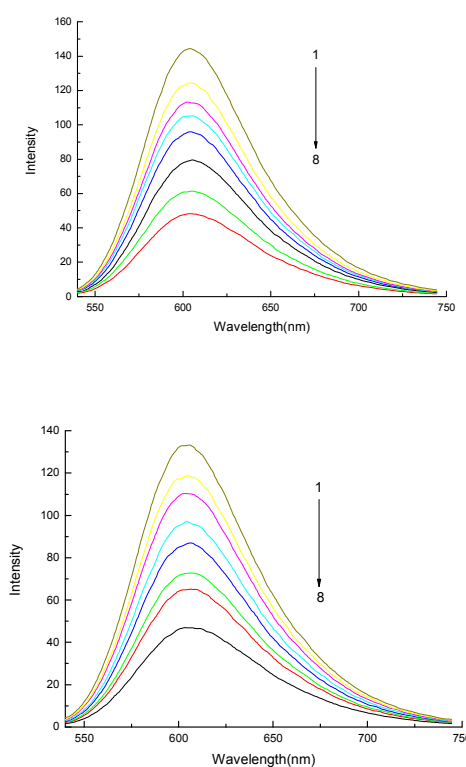
Figure.4. Fluorescence spectra of the binding of ethidium bromide to DNA in the absence (line 1) and presence (line 2–8) of increasing amounts of the complexes kex = 526 nm, C_{EtBr} = 1.0 μM, C_{DNA} = 5.1 μM, $C_{M(1–4)}$ (line 2–8): 2.5, 5.0, 7.5, 12.5, 25,37.5,50 (μM).

The fluorescence Scatchard plots obtained for competition of the complex (1 and 2) with EtBr to bind with DNA are given in Figure 6. The binding parameters for the fluorescence Scatchard plot of FS-DNA with EtBr in the presence of complexes are shown in Table 3. Obviously, the plot displays different affinity and binding site size. As shown in Figure 6, both complexes produce a Scatchard plot in which the slope decreases in the presence of increasing amounts of

complex, with little change in the intercept on the abscissa (0.1832 < x1 < 0.2197, 0. 1946 < x2 < 0.2107). They exhibit a type A behavior. (Type A behavior, competitive inhibition of ethidium binding, produces a Scatchard plot in which the slope decreases in the presence of increasing amounts of metal complex, with no change in the intercept on the abscissa (n).)[24,25]. It is possible to evaluate the observed association DNA binding constants. The results listed in Table 3 suggest that mononuclear metal intercalator owns more binding strengths with larger Kobs. The present results support this interpretation that intercalation can facilitate the covalent binding of the appropriate metal complexes to DNA.[25]

Table 3 Binding Parameters for the Fluorescence Scatchard Plot of FS-DNA with EtBr in the Presence of Complex **1** and **2** in Buffer at 20℃，$[DNA]_t/mol*L^{-1}=2.5\times10^{-5}$，$[M]_t/mol*L^{-1}=5\times10^{-6}$

Complex	$[E]_t$	F	F_0	C_E	r_E	r_M	C_M	K
1	2×10^{-6}	38.03	41.09	0.249×10^{-6}	0.07	0.15	1.125×10^{-5}	2.28×10^6
	3×10^{-6}	54.80	59.46	0.47×10^{-6}	0.15	0.119	1.202×10^{-5}	2.22×10^6
	4.5×10^{-6}	64.31	65.92	0.22×10^{-6}	0.1712	0.049	1.378×10^{-5}	1.56×10^6
2	2×10^{-6}	37.36	41.09	0.363×10^{-6}	0.0655	0.155	1.114×10^{-5}	3.75×10^6
	3×10^{-6}	52.85	59.46	0.667×10^{-6}	0.09332	0.127	1.183×10^{-5}	3.77×10^6
	4.5×10^{-6}	56.47	65.92	1.285×10^{-6}	0.129	0.091	1.273×10^{-5}	3.48×10^6

$[DNA]_t/mol*L^{-1}(2.5\times10^{-5})$ $[M]_t/mol*L^{-1}$ (5×10^{-6})
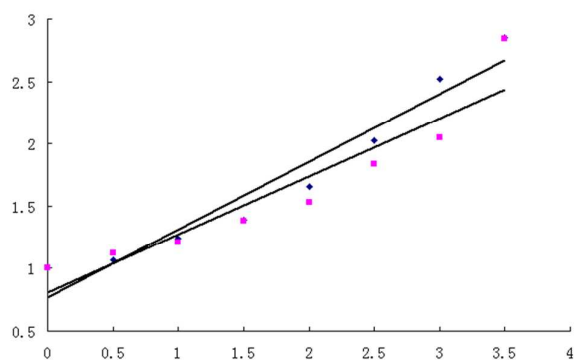
Figure. 5. Stern–Volmer quenching plots of the complex **1**, **2** with the value of slope 0.544 (complex 1), 0.465 (complex 2).
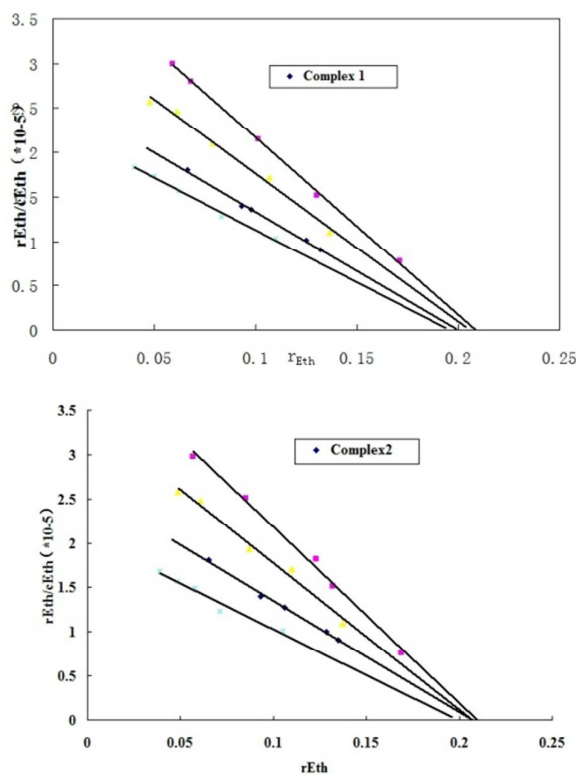
Figure 6. Fluorescence Scatchard plots for the binding of EtBr (0.5-5 M) to DNA in the absence and the presence of increasing concentrations of complexes 1 and 2.

Electronic absorption titration: The electronic absorption spectra is one of the most important ways and means for metal complexes to bind with DNA.[26–28] A complex bound to DNA through intercalation is characteristic of hypochromism and red shift due to the intercalative mode involving a strong interaction between an aromatic chromophore and the base pairs of DNA.[29] In Figure. 7, the absorption spectra of the two complexes in the absence and present of FS-DNA are illustrated. In the UV region, the complexes exhibit the intense absorption bands around 281 nm and 270 nm, respectively. These absorption bands are set down to the π-π* transition of the L ligands.[30] With increasing concentration of FS-DNA, the absorption bands of the complexes are affected, resulting in the slight tendency

of reduction in absorbency and red shift. The finding forebodes a strong stacking interaction between aromatic group and the base pairs of FS-DNA have taken place when the complexes intercalate to the FS-DNA. For enucleating action instance between the two complexes and FS-DNA, the intrinsic binding constant K of title complex with FS-DNA was determined according to the following equation[31], through a plot of [DNA]/(ε_a-ε_f) versus [DNA].[DNA]/(ε_a - ε_f) = [DNA]/(ε_b - ε_f) + 1/K(ε_b - ε_f). Intrinsic binding constant *K* of the two complexes was calculated to be about 1.69×10^5 M^{-1} and $1.15 \times 10^5 M^{-1}$, respectively. This K_b value is smaller than those reported for typical classical intercalators (EtBr–DNA, $3.3 \times 10^5 M^{-1}$ in 50 mM Tris–HCl/1.0 M NaCl buffer, pH 7.5).[32] The results are indicative of a weaker binding of DNA with the complexes than with the classical intercalators. It is logical to conjecture that interaction is comparatively strong between the complexes and FS-DNA.

The viscosity measurements were performed to further clarify insights about the mode of binding of the complexes to DNA. It is popularly accepted that a classical intercalation of a ligand into DNA is known to cause a significant increase in the viscosity of a DNA solution due to an increase in the separation of the base pairs at the intercalation site and, hence, an increase in the overall DNA molecular length; a partial and/or nonclassical intercalation of ligand could bend (or kink) the DNA helix, reduces its effective length and, concomitantly, its viscosity A plot of the relative specific viscositys ($\eta/\eta0$)$^{1/3}$ vs. binding ratio shows a significant change in the viscosity of DNA bound to the complexes 1 and 2. Figure. 8 shows the changes in viscosity on addition of complexes 1 and 2. On increasing the amounts of complexes 1 and 2, the relative viscosities of FS-DNA solution increase steadily. The increased degree of viscosity, which may depend on its affinity to DNA, followed the order of 1 > 2. The results indicate a partial intercalative binding nature of the complexes 1 and 2.

Figure. 7. Absorption spectrum of two complexes(**1** and **2**) in the absence and presence of increasing amounts FS-DNA ([complex] = 10μM, [DNA] = 0-48 μM). Arrow shows the absorbance changes upon increasing DNA concentration. Inset: plots of [DNA]/(ε_a -ε_f) versus [DNA] for the titration of DNA with the four complexes.
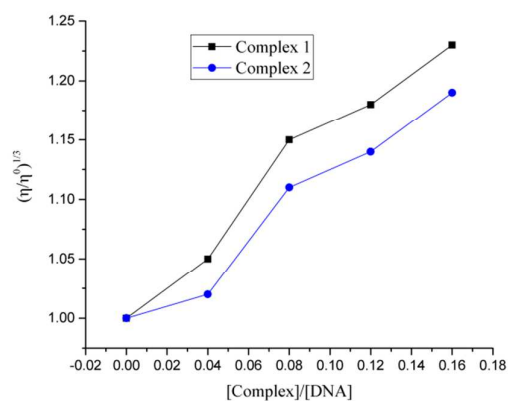
Figure. 8.Effect of increasing the concentration of the complexes 1 (■) and 2 (●) on the relative viscosities of CT DNA at 37.0(±0.1) ℃ in 5μm Tris–HCl buffer (pH 7.2).

Interaction of the complexes with N7，N3/N9 from the guanine and adenine： The major platination site

of cisplatin is known to be the N7 atom of guanine; this predominantly results in 1,2-d(GpG) intrastrand cross-links (65 %; p=linking phosphate group, dG=2'-deoxyguanosine). 1, 2-d (ApG) intrastrand, 1,3-d (GpNpG) intrastrand, and interstrand cross-links are formed to a minor extent (dA=2'-deoxyadenosine, dN=2'-deoxynucleoside).[33–38] Formation of intrastrand adducts was found to cause inhibition of DNA replication.[39] Chelation of different metal centers by the N7 atom and either the O^6 or the 6-NH_2 moiety of purine bases (guanine and adenine, respectively) has been suggested. In organometallic platinum(iv) chemistry, the crystal structure of a trimethylplatinum(iv)–theophylline hexamer with O^6–N7 chelation has been reported.[17] ^{1}H and ^{31}P NMR spectroscopy supported by molecular mechanics revealed that, instead of the O^6–N7 bidentate coordination, N7–αPO_4 macrochelation might occur during the reaction of cisplatin and 2'-deoxyguanosine 5'-monophosphate.[40, 41]

The ^{1}H NMR(DMSO-d_6, 300 MHz) data of the four title complexes with guanine are as follows:

complexes **1**: 6.51(s, 2H, H_2, H_2), 7.35(d, J=7.5 Hz, 1H, H_9), 8.56(d, J= 7.8 Hz, 1H, H_8) , 8.76(d, J= 7.5 Hz, 1H, H_d), 8.63(d, J= 7.5 Hz, 1H, H_e), 10.75(s, 1H, H_1); complexes **2**: 6.48(s, 2H, H_2, H_2), 7.36(d, J=7.5 Hz, 1H, H_9), 8.49(d, J= 7.8 Hz, 1H, H_8), 7.52(t, J= 8.1 Hz, 1H, H_b), 8.332(d, J= 5.7 Hz, 1H, H_a), 8.410(d, J= 6.3 Hz, 1H, H_c), 10.7(s, 1H, H_1).

complexes 3: 6.96(d, J=7.8 Hz ,2H, H_1, H_1), 7.936(t, J=7.5 Hz 1H, H_b), 8.342(d, J= 6.0 Hz, 1H, H_a) , 8.406(d, J= 5.4 Hz, 1H, H_c), 8.436(d, J= 6.9 Hz, 1H, H_2), 10.48(t, J=7.5 Hz,1H, H_1);

complexes 4:7.023(d, J=7.8 Hz ,2H, H_2, H_2), 8.25(d, J=7.2 Hz, 1H, H_2), 8.81(d, J= 7.5 Hz, 2H,H_d,

H_e),10.38(d, J=7.5 Hz, 1H, H_2).

By the analysis of the NMR data (including typical chemical shifts), a downfield of H_i is observed, Platination of 5'-GMP at the N7 position usually results in a downfield shift of the H8 proton (here H8 refers to H_i in this article) in the ^{1}H NMR spectrum, as shown in earlier studies, [42–45] indicating that the two complexes react with N7 position from the guanine respectively.

Interaction of the complexes with N3/ N9 from the adenine： In order to investigate the interaction of complex (1) with a DNA nucleobase, the crystal stucture of complex (2) was studied. The molecular structure of complex (2) is shown in Fig.4, together with atom numbering scheme. In the binuclear complex cation, each Pd(II) is chelated by one bipy ligand (coordinated by N1, N4), while the two Pd(II) cations are bridged by two ade ligands (one coordinated by N3, N9A, another, by N9, N3A). From Table 3 it can be seen that Pd(II) has a square-planar (distorted to rectangular) coordination geometry.The distance Pd1-Pd1A is 3.061A, indicating chemical metal–metal interaction [40]. The distances for the corresponding C…C contacts between the two bipy moieties are 4.258A, 4.713A, 4.551A, 3.883A, 3.460A, and 3.640A, the average distance being 4.084A, that may suggest intramolecular– stacking interaction which is slightly weaker than that (3.954A) previously observed in the paper [16]. The ^{1}H NMR(DMSO-d_6, 300 MHz) data of the two title complexes with adenine are as follows: free adenine: 10.33(s, 1H, H_1), 6.38(s, 2H, H_2, H_2), 7.28(d, J=7.5 Hz, 1H, H_9), 8.27(d, J= 7.8 Hz, 1H, H_8); complexes **1**: 6.51(s, 2H, H_2, H_2), 7.35(d, J=7.5 Hz, 1H, H_9), 8.56(d, J= 7.8 Hz, 1H, H_8) , 8.76(d, J= 7.5 Hz, 1H, H_d), 8.63(d, J= 7.5 Hz, 1H, H_e), 10.75(s, 1H, H_1); complexes **2**: 6.48(s, 2H, H_2, H_2), 7.36(d, J=7.5 Hz, 1H,

H$_9$), 8.49(d, J= 7.8 Hz, 1H, H$_8$), 7.52(t, J= 8.1 Hz, 1H, H$_b$), 8.332(d, J= 5.7 Hz, 1H, H$_a$), 8.410(d, J= 6.3 Hz, 1H, H$_c$), 10.7(s, 1H, H$_1$).

Many studies have been reported dealing with the binding mechanism of platinum complexes to DNA [41] and recently a class of palladium complexes containing bipy ligand has been reported [42, 43] but the mechanism of its action is not completely understood. In this paper the study on the hydrolysis kinetics of complex (1), synthesis and characterization of complex (2) provide more insight into the binding mechanism of these palladium complexes with DNA.
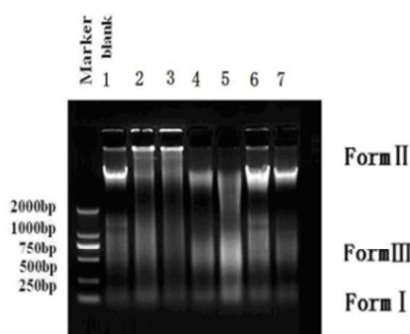
Figure. 9. Cleavage of FS-DNA in the presence of complexes, Lane 0, DNA alone; (lanes 1–7) in the different concentrations of the two complex [2-4: complex **1**, 5-7: complex **2**]

Cleavage of pBR322 plasmid DNA by complexes: The ability of complexes to perform DNA cleavage is generally examined by agarose gel electrophoresis.[44-48] The degree to which the two complexes could function as DNA-cleavage agents was measured using pBR322 plasmid DNA as the target. The two complexes **1** and **2** were established to promote the cleavage of pBR322 plasmid DNA from supercoiled Form (I) to the nicked Form (II) in Figure 9. Two clear bands were observed for the control in which the metal complex was absent (lane 0). The complexes can induce the cleavage of the pBR322 plasmid DNA at the concentration of 3.5 μM.

The amount of Form I of pBR322 plasmid DNA decreased gradually due to concentration increase of the two complexes, whereas Form II increased. On the other hand, the complexes showed different cleaving efficiency for the pBR322 plasmid DNA. The different DNA-cleavage efficiency of the complexes may be due to the different binding affinity of the complexes to DNA. [49-52]

Cytotoxicity in vitro study：The vitro cytotoxicity tests of the two complexes on selected human tumor cell lines were carried out. The IC$_{50}$ values are revealed in Table 4. In addition, Figure 10 shows the effect on cell growth after a treatment period of 72 h treatment with 3 μg/mL concentration. A viability rate by day 3 to less than 50% of the control values was observed for the complexes. On the whole, the Pt(II) complexes are effective in restraining the growth of HeLa and show a similar activity to cisplatin against the human tumor cell line, in descending order: complex **1**, cisplatin, complex **2**. The results are in accordance with IC$_{50}$ values.

Table 4 Cytotoxicity of the complexes against selected human tumor cells after 72 h of incubation

Tumor cells	In vitro activity (IC$_{50}$±SD, μM)		
	Complex **1**	Complex **2**	Cisplatin
Hela	0.63±0.05	0.84±0.08	0.73 ± 0.07
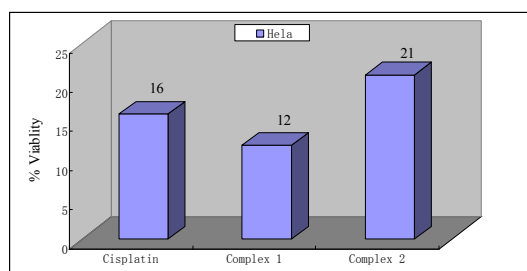
Figure. 10. Effect of 3μg/mL of the complex on HeLa cells viability after 72 h of incubation. All determinations are expressed as percentage of the control (untreated cells).

Apoptotic Study: Cell apoptosis is an autonomic ordered programmed cell death in order to maintain homeostasis, which is controlled by serial genes. Under the light microscope, the morphological changes of the HeLa cells have been observed.In figure.10a, the normal cells exhibited dense state and intercellular tight junction, single cell is Polygonal in shape or irregular cell morphology and cytoplasm is a clear appearance. After addition of the complexes (**1** and **2**), the cells appeared small size and became round in morphology comparing with normal cell and the state of being separated between them. As shown in Figure 11, the cells stained by hematoxylin-eosin were observed and the morphology of the cell nucleus have changed obviously. In Figure 11a, the nuclei of the normal cells were intact and had no pyknosis, which differed from the apoptotic cells, where the cell nucleus have become pyknotic (shrunken and dark) and condensed chromatin located on the nuclear membrane in Figure 11b-g. As stated previously, the two complexes have apoptosis on the HeLa cells apparently.
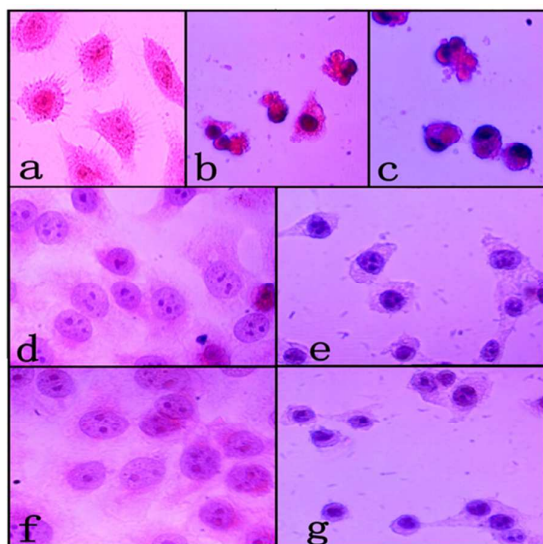
Figure.11. The morphological changes of the cells observed by light microscopy

To determine whether the inhibitory effects of complexes 1-2 on HL-60 cell viability resulted from apoptosis, we measured apop-totic processes by annexin V-FITC staining and propidium iodide(PI) accumulation, based on the early apoptotic phosphatidylserineresidue flip from the inner to outer surface of the cytoplasmic mem-brane, and analyzed cell staining by flow cytometry [53].

As the density plots in Figure 12 show, complexes 1-2 markedly increase the proportion of HL-60 cells with PS exposure (Annexin V+) and/or loss of plasma membrane integrity (PI+). Although the influence of these complexes on the PS exposure and loss of plasma membrane integrity varies in extent, the cell death induced by them follows a similar pathway, i.e. from the lower left quadrant (Annexin V−/PI−) to the lower right quadrant (Annexin V+/PI−) and then to the upper right quadrant (Annexin V+/PI+). Owing to complexes 1-2 induce HL-60 cancer cells to undergo the intermediate Annexin V+/PI− stage, the predominant death mode in this case is apoptosis. At a concentration of 100 mg/μl, complexes 1-2 was able to induce apopto-sis in HL-60 cells, with frequencies of 42.4% and 33.7%.We have found that the apoptotic effect of complexes with the order of **1**>**2**. This finding was consistent with our previous IC_{50} data.
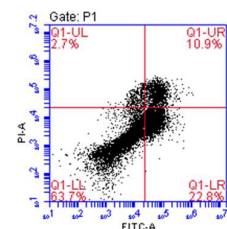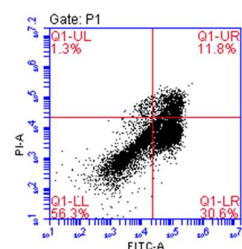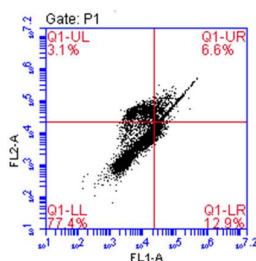
Figure.12. Flow cytometric analysis of HL-60 cells after incubation with Cisplatin and complexes 1-2 (10 mg/μl) for 12 h to detect annexinV-FITC staining.

Molecular docking

The method of molecule simulation is an efficient way to predict the correct binding mode and the interaction region. Targeting the minor groove of DNA through binding to a small molecule has long been considered an important tool in molecular recognition of a specific DNA-sequence. The rigid molecular docking studies were performed by using Autodock 4, an interactive molecular graphics program for calculating and displaying feasible docking modes of a pair of proteins, enzymes and DNA molecules. There were 3 H bonds between compounds and DNA without any p-p bond .According to figure 1,H bonds between O-G9,O-G8,N-G4 contribute to the intermolecular force ,meaning that the binding mode is non-covalent binding. The X-ray crystallographic structure of the human-DNA-Topo I complex (PDB ID: 1SC7) revealed that the Topo I is bound to the oligonucleotide sequence 5′-AAAAAGACTTsXGAAAATTTTT-3′, where 's' is 5′-bridging phosphorothiolate ofthe cleaved strand and 'X' represents any of the four bases A, G, C or T(Figure 13). The phosphoester bond of G12 in 1SC7 was rebuilt and SH of G11 on the scissile strand was changed to OH.
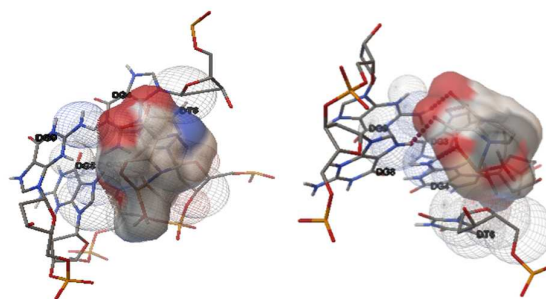
Figure.13. The minimum binding energy of the compounds is -6.74 kcal/mol (complex 1) -6.21kcal/mol (complex 2).

The binding energy of the first compound and the human telomeric was found to be -6.74kcal/mol by computation(Figure 14). Moreover, the second compound docked with the energy of -6.21kcal/mol. Thus, computer-aided molecular docking studies are in accordance with the experiment results.
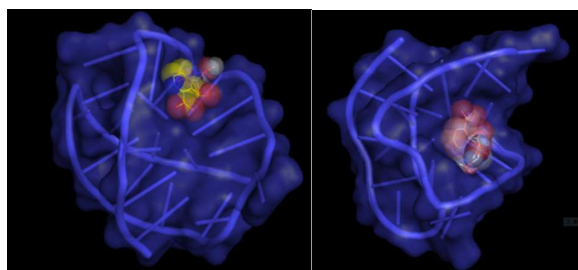
Figure.14. Binding mode of complex 1 and complex 2.

Experimental

Materials and methods: All chemicals and reagents purchased were of reagent grade and used without further purification unless otherwise noted. K_2PtCl_4 was of commercial origin. Pyrazine-2,3-dicarboxylic acid and Pyridine-2,3-dicarboxylic acid were obtained from commercial suppliers. The Hep-G2 cells, the KB cells and the AGZY-83a (human lung carcinoma) cells were obtained from American Type Culture Collection.

[Pt(L₁)(H₂O)₂](1): K_2PtCl_4 (41.51mg, 0.1mmol) was dissolved in water (10 mL) and in a separate beaker, ligand L_1 (16.81mg, 0.1mmol) was dissolved in water (10 mL). The platinum solution was slowly added

Journal Name ARTICLE

dropwise to the solution containing the ligand L_1 while stirring, and the mixture was allowed to react for 8 h at 45℃ in constant water bath. The solution was then filtered and kept in air. After a month, the resulting yellowish-green crystals were obtained then filtered, washed with aether and dried in vacuo. Complex 1 was prepared with a comparatively high yield (35.5 mg, 61%). Anal.Calcd. (%) for $C_6H_6N_2O_6Pt$ (1): C, 18.14; H, 1.52; N, 7.05. Found (%): C, 18.09; H, 1.59; N, 7.12; IR (cm^{-1}, s, strong; m, medium; w, weak): v(O-H) 3405(m); v(=C-H) 3098(m); v(C=O) 1673(m); v(C=C) 1571(m), 1440(m); v(C-N) 1347(m); v(C-O)1227(w); v(C-H) 745(w).^{1}H NMR (DMSO-d_6, 300 MHz)：8.807(d, J=7.2 Hz, 2H, H_d, H_e).

[Pt(L₂)(H₂O)₂]·H₂O(2): Complex 2 was synthesized in an ilk method as described in (1) with Pyridine-2,3-dicarboxylic acid (16.71 mg, 0.1 mmol) in place of Pyrazine-2,3-dicarboxylic acid. The product was obtained as a yellow-green crystals. Yield: 33.6 mg, 58%. Anal.Calcd. (%) for $C_7H_9NO_7Pt$ (1): C, 20.30; H, 2.19; N, 3.38. Found (%): C, 20.21; H, 2.23; N, 3.42; IR (cm^{-1}, s, strong; m, medium; w, weak): v(O-H) 3405(m); v(=C-H) 3099(s); v(C=O) 1674(m); v(C=C) 1527m), 1441(m); v(C-N) 1347(m); v(C-O) 1227 (m); v(C-H) 745(m).^{1}H NMR (DMSO-d_6, 300 MHz)：7.927(t, J=8.1 Hz, 1H, H_b), 8.322(d, J=5.7 Hz, 1H, H_a), 8.401(d, J=6.3 Hz, 1H, H_c).

Physical measurements： Elemental analysis (C, H and N) was performed on a model Finnigan EA 1112. The IR spectra was run as KBr pellets on Nicolet IR-470. The ^{1}H NMR spectra of DMs recorded on a Bruker Avance 300 MHz Spectrometer.

DNA-binding studies： Fluorescence measurements were obtained on a Perkin-Elmer LS55 fluorescence spectrofluorometer. For all fluorescence measurements, the entrance and exit slits were both maintained at 10 nm. The sample was excited at 526 nm and its emission appeared at 605 nm. The buffer used in the binding studies was 50 mM Tris–HCl, pH 7.4, containing 10 mM NaCl. The sample was incubated 4 h at room temperature (20 ℃) before spectral measurements. Under the conditions, the fluorescence intensity of the respective complexes, FS-DNA and ethidium bromide was significantly changed. The interaction of the respective Pt(II) complexes with DNA in vitro was studied as described in the literature.[54,55]

The fluorescence Scatchard plot was performed to study the binding constant determination by the luminescence titration method. Fixed amounts of DNA complex were titrated with increasing amounts of EtBr over a range of EtBr concentrations from 0.5 to 5 μM. An excitation wavelength of 526 nm was used, and the total fluorescence emission intensity was monitored at 605 nm. The experiments were conducted at 20℃ in a buffer containing 5mMTris-HCl (pH 7.1) and 50mMNaCl. Binding data were cast into the form of a Scathchard plot.[56] The concentration of the bound compound was calculated using the equation[57] $r_E/C= K(n- r_E)$, where C is the concentration of free ethidium, r is the ratio of bound complex to total nucleotide concentration [DNA], and n is the maximum value of r_E. The concentration of the free ethidium was calculated using the equation[58] $C=[(F\mathrm{max} - F)/(F\mathrm{max} - F_O)]C_{\mathrm{total}}$, where C_{total} is the total ethidium bromide concentration, F is the observed fluorescence emission intensity at a given EtBr concentration, Fmax is the intensity in the absence of complex, and F_O is the fluorescence of the totally bound complex. The plot of r_E/C versus rE gives the association constant (slope) and the constant binding

site size (x intercept) for the agents.

The viscometer was thermostated at 37 ℃ in a constant temperature bath. The concentration of DNA was 160 μM and the flow times were measured with an automated timer. Each sample was measured 3 times and an average flow time was calculated. The relative viscosities for FS-DNA in the presence and absence of the complex were calculated from the relation $\eta = (t - t_0)/t_0$, where t is the observed flow time of DNA-containing solution and t_0 is that of Tris–HCl buffer alone. Data were presented as $(\eta/\eta_0)^{1/3}$ $vs.$ binding ratio, where η is the viscosity of DNA in the presence of complexes and η_0 is the viscosity of DNA alone.[59]

Spectra were recorded on a UV-2550 double beam spectrophotometer. The absorption values were determined in the range 200–400 nm, using a 1 cm quartz cuvette. Samples were prepared in buffer (pH 7.4, 50 mM Tris–HCl, 10 mM NaCl) and analyzed at room temperature(20℃).

For the gel electrophoretic experiments, pBR322 plasmid DNA(0.33μg/μL) were treated with the platinum(II) complexes in Tris buffer (50 mM Tris–acetate, 18 mM NaCl buffer, pH 7.2), and the contents were incubated for 1 h at room temperature (20℃). The samples were eletrophoresed for 3 h at 90 V on 0.8% agarose gel in Tris–acetate buffer. After eletrophoresis, the gel was stained with 1 μg/mL ethidium bromide and photographed under UV light.

Cytotoxicity assay： The cytotoxicity of the four complexes was investigated on HeLa cells, the Hep-G2 cells, the KB cells and the AGZY-83a cells. IC$_{50}$ (the concentration of tested agent that caused 50% inhibition of cell growth) was determined using the MTT assay. This assay is based on the cleavage of the yellow tetrazolium salt (3-(4,5-dimethylthiazol-2-yl)-2,5-

diphenyl tetrazolium bromide; MTT, Sigma) forming purple formazan crystals by viable cells.[60] The cell lines were grown in 25 cm^2 tissue culture flasks in an incubator at 37 ℃ in a humidified atmosphere consisting of 5% CO$_2$ and 95% air. The cells were maintained in logarithmic growth phase in complete medium consisting of RPMI 1640, 10% (v/v) heat-inactivated fetal calf serum, 20 mM Hepes, 0.112% bicarbonate, and 2 mM glutamine. In short, the cells were seeded in a 96-well culture plate at 2×10^5 cells/well in a 100 μL culture medium and 24 h later they were exposed to tested compounds at different concentrations. The cells were incubated for 72 h. Then, 20 μL MTT solution (5 mg/mL) was added to each well and the cells were further cultivated for 4 h. After the removal of the medium, DMSO was added to each well to dissolve the formazan crystals, and the absorbance was determined at 450 nm. The IC$_{50}$ values were obtained from the results of quadruplicate determinations of at least three independent experiments.

Apoptotic assays by microscope: The HeLa cells in usable condition were seeded in a 24-well culture plate at 2×10^5 cells/well in a 1 mL culture medium and 24 h later the medium including the Pt(Ⅱ) complexes was given. The concentration of the two complexes was 1 μM/mL. The cells were further incubated for 48 h, then the level of apoptosis was evaluated at least three independent experiments. The hematoxylin-eosin stain was the means of the apoptotic morphology observed by light microscopy.[61] Under the light microscope, the cytoplasm had been stained pink and with blue-black in the nucleolus.

Apoptosis assays by flow cytometry: The ability of complexes 1-2 to induce apoptosis is evaluated in HL-

60 cells line using Annexin V conjugated with FITC and propidium iodide (PI) counterstaining by flow cytometry. The HL-60 cell cells in a usable condition were seeded in a 6-well culture plate at 1×106 cells per well in a 3mL culture medium and 12h later the medium including the complexes 1-4 was given. After 12h incubation, cells were gathered, wash cells twice with cold phosphate-buffered saline (PBS) and then resuspend cells in 1X Binging Buffer at a concentration of 1×10^6 cells/ml. Transfer 100μL of the solution (1×10^5 cells) to a 5ml culture tube. Add 5μL of FITC Annexin V and 5μL PI. Gently vortex the cells and incubate for 15min at RT (25°C) in the dark. Add 400μL of 1X Binding Buffer to each tube. Analyze by flow cytometry（Accuri C6, USA）within 1 hr.

Molecular docking

The change of transcription or replication of DNA may lead to gene mutation, thus causing a series of diseases, in this way it plays an irreplaceable role in life. DNA is also the target of many antiviral, cancer and antibacterial drugs, playing a significant role in the treatment of diseases. The study of interaction of small molecules and DNA can express carcinogens' carcinogenic properties, contributing to further understanding of the molecular mechanisms of drug, as well as the drug–DNA interactions in rational drug design.[62] The big grooves and small grooves are the mainly binding sites of DNA. The interaction of binding mode can be non-covalent binding, covalent binding, long-range assembly. The first step is to explore the interaction of the binding model of the series of compounds and DNA molecule. Then the binding energy must be calculated. Structures of the series of compounds were drawn CHEMDRAW and converted into pdb format from mol format by CHEM3D. The crystal structures of the B-DNA dodecamer

d(CGCGAATTCGCG)2 (PDB ID: 1BNA) and the human telomeric complex (PDB ID: 143D.) were downloaded from the protein data bank . Visualization of the docked pose has been done by using PyMol molecular graphics program.

X-ray crystal structure measurement for the complex 1 and 2：Single-crystal data of the two complexes were collected at 293 K the range of $2.49 \leq \theta \leq 25.38$ or $2.21 \leq \theta \leq 25.66$ on a Brucker Smart 1000 CCD diffractometer with MoKa radiation (k = 0.71073 13). The structures were solved by direct methods with SHELXL 97[63] and refined by means of the full-matrix least squares procedures on F^2. All non-hydrogen atoms were refined anisotropically. Hydrogen atoms were included at ideal geometrical positions. Structure solution and refinement based on 1,684 or 1,882 independent reflections with $I > 2\sigma(I)$ gave R1=0.0182, wR2=0.0460 or R1 = 0.0217, wR2 = 0.0536. The CCDC number of the crystal complexes **1** and **2** is 755873 and 755874, respectively.

Conclusions

The two novel complexes were developed and evaluated in bioassays for potential further development toward novel anticancer agents. The DNA-binding properties of the complexes were examined by absorption and fluorescence spectra. The results support the fact that the complexes bind to DNA with different bonding effects. The capability of cleavage of FS-DNA by the complexes is investigated by agarose gel electrophoresis, the results indicate that the complexes exhibit an efficient DNA-cleavage. Cytotoxic and antiproliferative studies show that the two complexes exhibit good cytotoxic activity against HeLa cell lines tested. Additionally, the apoptotic tests indicated that the

complexes had an apoptotic effect on HeLa cells. Molecular dynamic simulations molecular docking studies focused on binding modes and has given less ambiguous visual pictures which supported all experimental results as complex 1 > complex 2. Encouraging chemical and biological findings indicate that these complexes are very promising candidates as live-cell imaging reagents that could contribute to the understanding of cellular uptake of metal complexes.

Acknowledgements

Notes and references

1 (a)Rosenberg, B. *in: H. Sigel (Ed.), Metal Ions in Biological Systems, vol. II, Marcel Dekker, New York,* 1980; pp 127;(b) J. Reedijk, Chem. Rev., 1999, 99, 2499.

2 (a)M. L. Jain, P. Y. Bruice, I. E. Szabó and T. C. Bruice, *Chem. Rev.,* 2012, **112**, 1284; (b) I. Eryazici, C. N. Moorefield and G. R. Newkome, *Chem. Rev.,* 2008, **108**, 1834;

3 Chu,G. *J. Biol. Chem.,* 1994, **269**,787.

4 (a)S. P. Fricker, *Metallomics,* 2010, **2**, 366; (b) C. G. Hartinger, N. Metzler-Nolte and P. J. Dyson, *Organometallics,* 2012, **31**, 5677.

5 (a)G. Zhu, M. Myint, W. H. Ang, L. Song and S. J. Lippard, *Cancer Res*., 2012, **72**, 790;(b)P. M. Takahara, C. A. Frederick and S. J. Lippard, *J. Am. Chem. Soc.,* 1996, **118**, 12309; (c) K. S. Lovejoy, et al., *Proc. Natl. Acad. Sci.* U. S. A., 2008, **105**, 8902.

6 (a) M. Zampakou, S. Balala, F. Perdih, S. Kalogiannis, I. Turelc, G.Psomas, *RSC Adv*. 2015, **5**, 11861;(b) Z.L. Yuan, X.M. Shen, J.D. Huang, *RSC Adv*. 2015, **5**, 10521; (c) Kallappa. M. Hosamani, Dinesh S. Reddy, Hirihalli. C. Devarajegowd, *RSC Adv*. 2015, **5**, *11261;(d)* H.L. Jia, Y. Lv, S. Wang, D. Sun, L.Y Wang, *RSC Adv*. 2015, **5**, 4681;

7 N. J. Wheate, S. Walker, G. E. Craig and R. Oun, *Dalton Trans.,* 2010, **39**, 8113.

8 Y. W. Jung and S. J. Lippard, *Chem. Rev.,* 2007, **107**, 1387.

9 Gao, E. J.; Wang, L.; Zhu, M. C.; Liu, L.; Zhang, W, Z. *Eur. J. Med. Chem*. 2010, **45**, 311.

10 Gao, E. J.; Zhu, M. C.; Liu, L.; Zhang, W, Z. Huang, Y.; Wang, L., Shi, C. Y.; Zhang, W. Z.; Sun, Y. G. *Inorg. Chem*. 2010, **49**, 3261.

11 Reeder, F; Guo, Z; Murdoch, P. del S; Corazza, A; Hambley, T. W; Berners-Price, S. J; Chottard, J.C; Sadler, P. J. *Eur. J. Biochem.* 1997, **249**, 370.

12 Barnham, K. J; Berners-Price, S. J; Frenkiel, T. A; Frey, U; Sadler, P. J. *Angew. Chem.* 1995, 107, 2040-2043; *Angew. Chem. Int. Ed. Engl.* 1995, **34**, 1874.

13 Fichtinger-Schepman,A. M; van der Velde-Visser, S. D; van Dijk-Knijnenburg, H. C. M; van Oosterom, A. T; Baan, R. A; Berends, F. *Cancer Res.*1990, **50**, 7887.

14 Legendre, F; Bas, V; Kozelka,J; Chottard, J.C. *Chem. Eur. J.* 2000, **6**, 2002.

15 Monjardet-Bas, V; Chottard, J.C; Kozelka, J. *Chem. Eur. J.* 2002, **8**, 1144.

16 Szalda, D. J; T. Kistenmacher, J; Marzilli, L. G. *J. Am. Chem. Soc.* 1976, **98**, 8371.

17 Lorberth, J; El-Essawi, M; Massa, W; Labib, L. *Angew. Chem*. **1988**, **100**, 1194.

18 Janiak, C.*J. Chem. Soc. Dalton Trans.* 2000, **24**, 3885.

19 Yang, B.S; Feng, J.Y; Li, Y.Q; Gao, F; Zhao, Y.Q; Wang, J.L. *J. Inorg. Biochem.* 2003, **96**, 416.

20 Baguley, B.C; Le Bret, M. *Biochemistry.* 1984, **23**, 937.

21 Gao, E. J.; Wang, L.; Zhu, M. C.; Liu, L.; Zhang, W, Z. Eur. J. Med. Chem. 2010, **45**, 311.

22 Liu, J; Zhang, T.X; Lu, T.B; Qu, L.H; Zhou, H; Zhang, Q.L; Ji, L.N. *J. Inorg. Biochem.*2002, **91**, 269.

23 Marianthi Z.; Sofia Balala.; Franc Perdih.; Stavros Kalogiannis.; Iztok Turel.; George Psomas. *RSC Adv.*,2015, **5**, 11861.

24 Arakawa, H.; Ahmad, R.; Naoui, M.; Tajmir-Riahi, H. A. *J. Biol. Chem.* 2000, **275**, 10150.

25 Howe-Grant, M.; Wu, K. C.; Bauer, W. R.; Lippard, S. *J. Biochemistry.* 1976, **15**, 4339.

26 Zhang, Q.L; Liu, J.G; Liu, J.Z; Li, H; Yang, Y; Xu, H; Chao, H; Ji, L.N.

Inorg. Chim. Acta. 2002, **339**, 34.

27 Zhang, Q.L; Liu, J.G; Chao, H; Xue, G.Q; Ji, L.N. *J. Inorg. Biochem.* 2001, **83**, 49.

28 Zou, X.H; Ye, B.H; Li, H; Liu, J.G; Xiong, Y; Ji, L.N. *J. Chem. Soc., Dalton Trans*. 1999, **9**, 1423.

29 Kumar, R. S; Sasikala, K；Arunachalam, S. *J. Inorg. Biochem.* 2008, **102**, 234.

30 He, X.F; Wang, L; Chen, H; Xu, L; Ji, L.N. *Polyhedron* 1998, **17**, 3161.

31 Wolfe, A; Shimer, G.H. T. *Meehan, Biochemistry.* 1987, **26**, 6392.

32 Strothkamp, K.G; Strothkamp, R.E. *J. Chem. Edu.* 1994, **71**, 77.

33 Fichtinger-Schepman, A. M; Lohman, Reedijk, P. H. *J. Nucleic Acids Res.* 1982, *10*, 5345.

34 Fichtinger-Schepman, A. M; van der Veer, J. L; den Hartog, J. H; ;Lohman, P. Reedijk, H. *J. Biochemistry.* 1985, *24*, 707.

35 Pinto, A. L; Lippard, S. *J. Biochim. Biophys. Acta.* 1985, **780**, 167.

36 Eastman, A. *Biochemistry.* 1982, **21**, 6732.

37 Jamieson, E. R; Lippard, S. *J. Chem. Rev*. 1999, **99**, 2467.

38 Sherman, S. E; Lippard, S. *J. Chem. Rev*. 1987, **87**, 1153.

39 Gralla, J. D; Sasse-Dwight, S; Poljak, L. G. *Cancer Res.* 1987, **47**, 5092.

40 Reily, M. D; Marzilli, L. G. *J. Am. Chem. Soc.* 1986, **108**, 6785.

41 Reily, M. D; Hambley, T. W; Marzilli, L. G. *J. Am. Chem. Soc.* 1988, **110**, 2999.

42 Bloemink, M. J; Lempers, E. L. M; Reedijk, J. *Inorg. Chim. Acta*. 1990, **176**, 317.

43 Berners-Price, S. J; Frenkiel, T. A; Ranford, J. D; Sadler, P. J. *J. Chem. Soc.-Dalton Trans*. 1992, **13**, 2137.

44 Kiser, D; Intini, F. P; Xu, Y. H; Natile, G; Marzilli, L. G. *Inorg. Chem*. 1994, **33**, 4149.

45 Jansen, B. A. J; van der Zwan, J; Reedijk, J; den Dulk, H. J. Brouwer, *Eur. J. Inorg. Chem*. 1999, **9**, 1429.

46 Moreno, R.G.M; Alipa´zaga, M.V; Gomes, O.F; Linares, E; Medeiros, M.H.G; Coichev, N. *J Inorg Biochem*. 2007, **101**, 866.

47 Macı´as, B; Villa, M.V; Go´mez, B; Borra´s, J.;Alzuet, G. ; Gonza´lez-A´lvarez, M;CastiNˇeiras. A. *J. Inorg. Biochem*. 2007, **101**, 444.

48 Ghosh, S; Barve, A.C; Kumbhar, A.A; Kumbhar, A.S; Puranik, V.G; Datar, P.A; Sonawane, U.B; Joshi, R.R. *J. Inorg. Biochem*. 2006, **100**, 331.

49 (a) E. J. Gao, C. Liu, M. C. Zhu, H. K. Lin, Q. Wu and L. Liu, *Anti-*

Cancer Agents in Medicinal Chemistry, 2009, **9**, 356; (b)L. Giovagnini, L. Ronconi, D. Aldinucci, D. Lorenzon, S. Sitran, D. Fregona, *J. Med. Chem.*, 2005, **48(5)**, 1588; (c)A. G. Quiroga, C. N. Ranninger, *Coord. Chem. Rev.,* 2004, **248(1-2)**, 119; (d) S. Ray,

R. Mohan, J. K. Singh, M. K. Samantaray, M. M. Shaikh, D. Panda, P. Ghosh, *J. Am. Chem. Soc.,* 2007, **129(48)**, 15042;

50 Gao, E.J; Wang, K.H; Gu, X.F; Yu, Y; Sun, Y.G; Zhang, W.Z ; Yin, H.X;

Wu, Q; Zhu, M.C; Yan, X.M. *J. Inorg. Biochem.* 2007, **101**, 1404.

51 Wang, X.L; Chao, H; Li, H; Hong, X.L; Liu, Y.J; Tan, L.F; Ji, L.N. *J. Inorg. Biochem*. 2004, **98**, 1143.

52 Qian, J；Gu, W；Liu, H；Gao, F.X.；Feng, L；Yan, S.P；Liao, D.Z；Cheng, P. *Dalton Trans.* 2007, **10**, 1060.

53 A. Eastman, *Cancer Cells.* 1990, **2**, 275.

54 Mital, R; Srivastava, T.S. *J. Inorg. Biochem.* 1990, **40**, 111.

55 Vital, R; Srivastava, T.S; Parekh, H.K; Chitnis, M.P. J. Inorg. Biochem. 1991, **41**, 93.

56 Satyanarayana, S.; Dabrowiak, J. C.; Chaires, J. B. *Biochemistry.* 1992, **31**, 9319.

57 B. S. Yang, J. Y.Feng, Y. Q. Li, F. Gao, Y. Q, Zhao, J. L. Wang, *J. Inorg. Biochem*. 2003, **96**, 416.

58 Kumar, C. V.; Asuncion, E. H. *J. Am. Chem. Soc*. 1993, **115**, 8547.

59 (a)Cohen,G., Eisenberg, H., *Biopolymers*, 1969, **8**, 45; (b) Satyanarayana, S., Dabrowiak, J. C., Chaires, J. B., *Biochemistry,* 1993, **32**, 2573.

60 M. C. Alley, D. A. Scudiero, A. Monks, M. L. Hursey, M. J. Czerwinski, D. L. Fine, B. J. Abbott, J. G. Mayo, R. H. Shoemaker, M. R. Boyd, *Cancer Res*. 1988, **48**, 589.

61 J.L. García-Giménez, M. González-Álvarez, M. Liu-González, B. Macías, J. Borrás, G. Alzuet, *J. Inorg. Biochem.* 2009, **103**, 923.

62 Koyel Misra, Goutam Kr Ghosh, Ishani Mitra, Subhajit Mukherjee, Venkata P. Reddy B., Wolfgang Linert, Bashkim Misini, Jagadeesh C. Bose K, Sudit Mukhopadhyay, Sankar Ch Moi, *RSC Adv.*2015, **5,** 12454.

63 (a) G. M. Sheldrick, SHELXS 97: Program for the Solution of Crystal Structures, University of Gottingen. 1997; (b)G. M. Sheldrick, SHELXL 97: Program for the Refinement of Crystal

Structures, University of Gottingen. 1997;(c) G. M. Sheldrick,

Acta Cryst. A 2008, **64**, 112.